Targeting Extracellular Domains D4 and D7 of Vascular Endothelial Growth Factor Receptor 2 Reveals Allosteric Receptor Regulatory Sites

MCB
Journals.ASM.org

Targeting Extracellular Domains D4 and D7 of Vascular Endothelial Growth Factor Receptor 2 Reveals Allosteric Receptor Regulatory Sites

Caroline A. C. Hyde,[a] Alexandra Giese,[a] Edward Stuttfeld,[a]* Johan Abram Saliba,[b] Denis Villemagne,[b] Thomas Schleier,[a] H. Kaspar Binz,[b] and Kurt Ballmer-Hofer[a]

Paul Scherrer Institute, Biomolecular Research, Molecular Cell Biology, Villigen PSI, Switzerland,[a] and Molecular Partners AG, Zürich-Schlieren, Switzerland[b]

Vascular endothelial growth factors (VEGFs) activate three receptor tyrosine kinases, VEGFR-1, -2, and -3, which regulate angiogenic and lymphangiogenic signaling. VEGFR-2 is the most prominent receptor in angiogenic signaling by VEGF ligands. The extracellular part of VEGF receptors consists of seven immunoglobulin homology domains (Ig domains). Earlier studies showed that domains 2 and 3 (D23) mediate ligand binding, while structural analysis of dimeric ligand/receptor complexes by electron microscopy and small-angle solution scattering revealed additional homotypic contacts in membrane-proximal Ig domains D4 and D7. Here we show that D4 and D7 are indispensable for receptor signaling. To confirm the essential role of these domains in signaling, we isolated VEGFR-2-inhibitory "designed ankyrin repeat proteins" (DARPins) that interact with D23, D4, or D7. DARPins that interact with D23 inhibited ligand binding, receptor dimerization, and receptor kinase activation, while DARPins specific for D4 or D7 did not prevent ligand binding or receptor dimerization but effectively blocked receptor signaling and functional output. These data show that D4 and D7 allosterically regulate VEGFR-2 activity. We propose that these extracellular-domain-specific DARPins represent a novel generation of receptor-inhibitory drugs for *in vivo* applications such as targeting of VEGFRs in medical diagnostics and for treating vascular pathologies.

Receptor tyrosine kinases (RTKs) accomplish essential functions in a wide variety of biological processes, such as cell growth, differentiation, migration, and survival. Vascular endothelial growth factors (VEGFs) are a family of proteins that interact with three type V RTKs, VEGFR-1 (Flt-1), VEGFR-2 (KDR/Flk-1), and VEGFR-3 (Flt-4) (reviewed in reference 15). VEGFs promote endothelial cell survival, migration, proliferation, and differentiation and are thus indispensable for blood and lymph vessel formation and homeostasis. In addition, VEGFs regulate endothelial cell permeability and vessel contraction (8). Like all RTKs, VEGFRs are activated upon ligand-induced structural changes in the receptor extracellular domain (ECD) that instigate transmembrane signaling (reviewed in reference 25). VEGFR-2 is the major mediator of VEGF signaling in endothelial cells, and its activity is regulated at multiple levels. We have shown recently that receptor dimerization is necessary but not sufficient for VEGFR-2 kinase activation (7), suggesting that precise orientation of receptor monomers in active dimers is critical to the instigation of transmembrane signaling. In addition, biochemical data (9, 24) and high-resolution structural information for VEGF ligand/receptor complexes (6, 17) revealed that extracellular immunoglobulin homology domains (Ig domains) D2 and D3 (D23) comprise the ligand binding site. Furthermore, structural information derived from electron microscopy (EM) (22) and small-angle X-ray scattering (SAXS) data (14) suggests that the ligand-bound VEGFR-2 ECD is also engaged in homotypic contacts between Ig domains D4 and D7. The putative contacts in D7 were further confirmed by X-ray crystallography, which showed that charged residues in the βE-F loop promoted D7 dimerization (28) (Fig. 1B). We have recently demonstrated that homotypic receptor contacts are enthalpically unfavorable and reduce the overall binding activity of the ligand for VEGFR-2 (6). Taken together, these data suggest that the two monomers comprising the active receptor complex are held together by ligand binding to Ig domains 2 and 3 (D23) and by homotypic receptor contacts in D4 to D7 of the ECD. We assume that these interactions are essential for correct positioning of receptor monomers in active dimers and that the enthalpic penalty that arises from these interactions may perform a proofreading function that prevents inappropriate receptor activation in the absence of a ligand.

Here we further investigate the role of Ig domains D4 and D7 in receptor activation and downstream signaling and show that the mutation of these domains drastically reduces receptor activity. To confirm the role of D4 and D7 in receptor activation, we selected designed ankyrin repeat proteins (DARPins) that specifically interact with the VEGFR-2 ECD. DARPin interaction with D23 blocked ligand binding, receptor dimerization, and activation, while interaction with D4 or D7 inhibited receptor activity without blocking dimerization, thus revealing a new allosteric receptor-inhibitory mechanism. These highly specific receptor binders have potential for *in vivo* clinical applications such as vascular imaging or for therapeutic antiangiogenic targeting of VEGFR-2 in tumor microenvironments or in retinopathies.

MATERIALS AND METHODS

Antibodies and chemicals. Primary antibodies directed toward phospho-VEGFR-2 (p-Tyr1175, p-Tyr1214, p-Tyr951), phospho-phospholipase Cγ-1 (p-PLCγ-1), VEGFR-2, and PLCγ-1 (PLCγ-1) were purchased from Cell Signaling Technology (BioConcept, Allschwil, Switzerland); an

Received 28 December 2011 Returned for modification 26 January 2012
Accepted 6 July 2012
Published ahead of print 16 July 2012
Address correspondence to Kurt Ballmer-Hofer, kurt.ballmer@psi.ch.
Present address: Edward Stuttfeld, Biozentrum, University of Basel, Basel, Switzerland.
C.A.C.H., A.G., and E.S. contributed equally to this paper.

doi:10.1128/MCB.06787-11

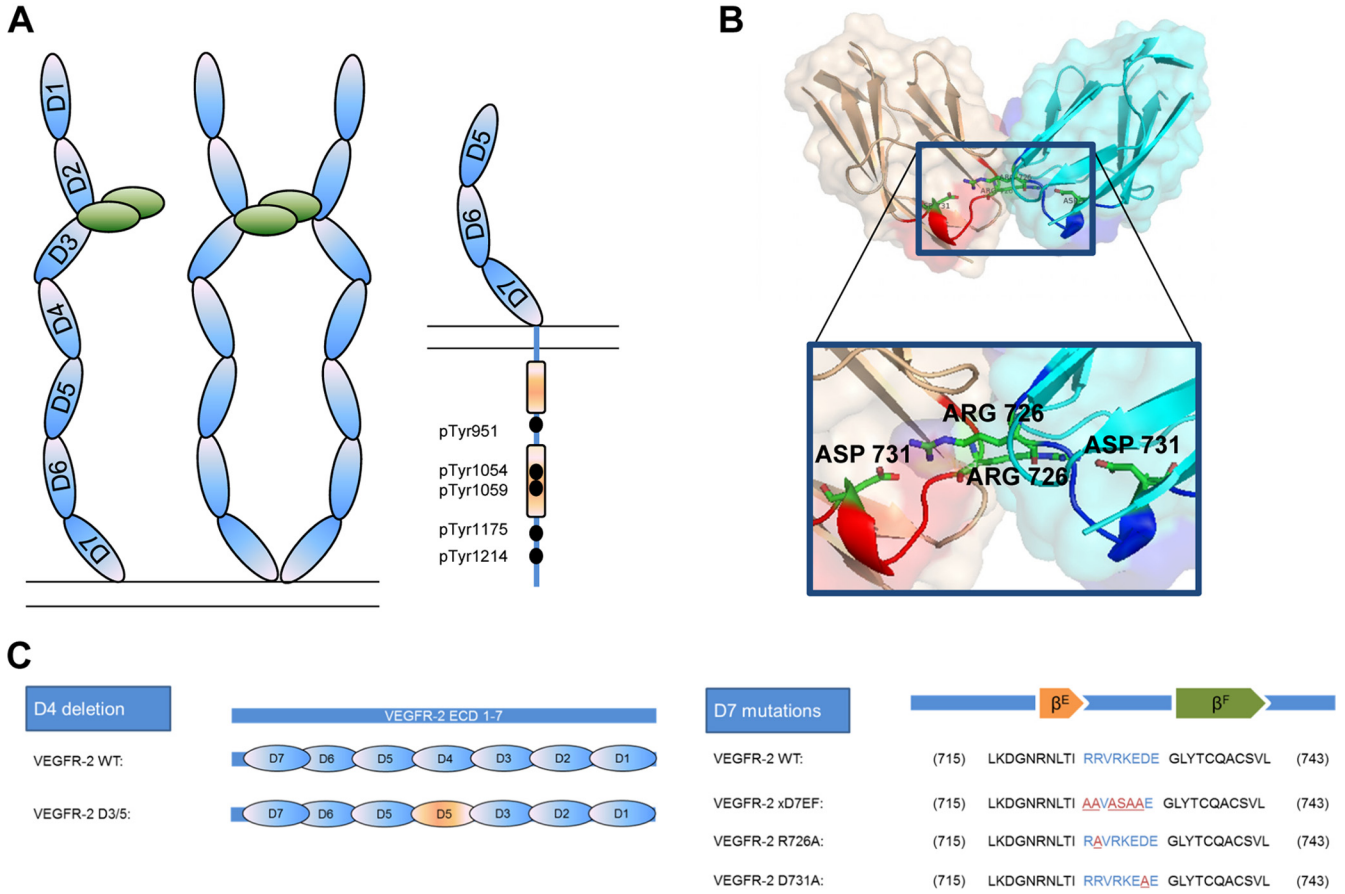

FIG 1 Schematic representation of VEGFR-2 structure and diagrams of mutant VEGFR-2 constructs. Schematic representation of the VEGFR-2 structure (A) and structural model of the D7 dimer of VEGFR-2 (B) generated with PyMol (www.PyMol.org) from the coordinates of the X-ray structure with Protein Data Bank code 3KVQ (28). The βE-F loop in the monomers are enhanced by darker coloring, and aspartate 731 and glutamate 726, which form hydrogen bonds between the adjacent monomers, are labeled. (C) Sequences of receptor mutant constructs used in Fig. 2.

antibody directed toward p-Tyr1054/59 was from Merck Calbiochem, Zug, Switzerland. Antibodies directed toward tubulin and VEGFR-2 ECD (ab11939) were from Abcam, Cambridge, United Kingdom. Alkaline phosphatase (AP)-conjugated AffiniPure goat anti-rabbit and anti-mouse IgGs were purchased from Jackson ImmunoResearch (Milan Analytica AG, Magden, Switzerland). Mouse anti-Myc tag antibody was from R&D Systems Europe Ltd. (Abingdon, United Kingdom), and mouse anti-RGS-His antibody was from Qiagen AG (Basel, Switzerland). Lumi-Phos Western blotting reagent was from Thermo Fischer Scientific, Basel, Switzerland. Roti polyvinylidene difluoride (PVDF) membranes were from Carl Roth GmbH & Co. KG, Karlsruhe, Germany. Complete protease inhibitor cocktail was from Roche Diagnostics GmbH (Rotkreuz, Switzerland), and all PCR primers were purchased from Microsynth AG (Balgach, Switzerland). Rat tail collagen type I was obtained from BD Biosciences, San Jose, CA. All solvents and chemicals were of analytical grade.

Cell culture. Human embryonic kidney epithelial 293 cells (HEK293 [11] and HEK293T [12]) and bovine aortic endothelial cells (BAEC; generously supplied by R. Montesano, University of Geneva, Geneva, Switzerland [21]) were grown in Dulbecco's modified Eagle's medium (DMEM; BioConcept, Basel, Switzerland) supplemented with 10% fetal bovine serum (FBS) or 10% newborn calf serum (NCS), respectively. Porcine aortic endothelial cells (PAEC) were maintained in Ham's F12 medium (BioConcept) containing 10% FBS. Cells were grown in a humidified atmosphere at 37°C and 5% CO_2. Sf21 insect cells were maintained in serum-free Insect-Express medium (Lonza, Basel, Switzerland) at 27°C.

Plasmid construction. All mammalian receptor mutant constructs were generated by PCR subcloning (10) into the pcDNA5FRT vector (Invitrogen, Carlsbad, CA) using wild-type (WT) pcDNA3_VEGFR-2 as the template. Expression plasmids for soluble ECD recombinant protein production in HEK293 cells were generated by PCR subcloning from pcDNA3_VEGFR-2 ECD (23). For insect cell expression of VEGFR-2 ECD proteins, we used pFASTBAC (Invitrogen) as an entry vector to generate baculoviruses.

Recombinant proteins. VEGFR-2 ECD protein was produced and purified as described previously (17). Briefly, Sf21 cells at a density of 1×10^6/ml were infected with recombinant baculovirus. Three days postinfection, supernatant was harvested, cleared by centrifugation, concentrated, and dialyzed against 20 mM sodium phosphate buffer (pH 7.4), 500 mM NaCl. Culture supernatants were further purified by immobilized metal affinity chromatography (IMAC) using a Ni^{2+}-nitrilotriacetic acid agarose column (GE Healthcare). His_6-tagged proteins were eluted with a gradient of 40 to 500 mM imidazole and further purified by gel filtration on Superdex 200HR 10/30 (GE Healthcare) equilibrated with 25 mM HEPES (pH 7.5), 150 mM NaCl. VEGFR-2 ECD proteins encompassing D7, D1 to D3, or D2 to D4 and VEGFR-1 ECD D1 to D7 were produced in transiently transfected HEK293T cells as described previously (2). At approximately 90% confluence, the cells were incubated in DMEM with 0.5% FBS together with a DNA-polyethylenimine (PEI) complex at a wt/wt ratio of 1:1.5 (25-kDa PEI; Sigma-Aldrich, St. Louis, MO). Three days after transfection, supernatants were harvested, cleared by centrifugation, and concentrated. The buffer was then exchanged to 25 mM HEPES (pH 7.5), 150 mM NaCl using centrifugal protein concen-

trators (Sartorius Stedim Biotech, Aubagne, France), and the His_6-tagged proteins were purified by IMAC as described above.

Transient and stable transfections. PAEC and HEK293 cells were transfected with FuGENE HD transfection reagent (Roche, Switzerland) according to the manufacturer's protocol. To establish stable PAEC, cells were selected with 1 mg/ml Geneticin (Merck Calbiochem, Zug, Switzerland) for 2 weeks and then subcloned.

Western blotting. Cells were serum starved in DMEM supplemented with 1% bovine serum albumin (BSA) and stimulated with 1.5 nM VEGF-A_{165} for 10 min at 37°C with or without 45 min of preincubation with DARPin (0.1 to 1 μM). Cell lysates were prepared in lysis buffer (50 mM Tris [pH 7.5], 100 mM NaCl, 0.5% [wt/vol] Triton X-100) supplemented with protease inhibitor cocktail, phosphatase inhibitors (200 μM Na_3VO_4, 10 mM NaF, 10 mM sodium pyrophosphate, 30 mM *p*-nitrophenylphosphate, 80 mM glycerophosphate, and 20 μM phenylarsine oxide), and 10% glycerol. Washed immunoprecipitates were boiled in Laemmli buffer (20 mM Tris [pH 6.8], 5% SDS, 10% mercaptoethanol, 0.02% bromphenol blue), resolved by 8% SDS-PAGE, transferred to PVDF membranes, and immunodecorated with primary antibodies (dilution, 1:1,000) followed by secondary alkaline phosphatase-coupled antibodies (1:10,000), and developed with Lumi-Phos. Immunoblot assays were analyzed with a GE Healthcare ImageQuant RT ECL scanner and densitometrically quantified with ImageQuant TL software (version 7.0; GE Healthcare Europe GmbH, Glattbrugg, Switzerland).

Immunofluorescence microscopy. HEK293 cells or stably transfected PAEC were grown on glass coverslips to 60% confluence. Cells were fixed with 3.7% formaldehyde in phosphate-buffered saline (PBS) for 10 min at 37°C, permeabilized for 10 min with 1% NP-40 in PBS (wt/vol), and blocked for 20 min in 5% (wt/vol) BSA in PBS at room temperature (RT). Samples were sequentially exposed at RT to ECD binders (30 μg/ml) and primary (1:500) and fluorescently labeled secondary (1:1,000) antibodies in PBS containing 1% BSA and embedded in Gelvatol (15% Gelvatol [Celanese Corporation, Lanaken, Belgium], 33% glycerol, 0.1% sodium azide). Cells were extensively washed with PBS after each step. Images were acquired with an Olympus IX81 epifluorescence microscope at ×60 magnification and processed by using three-dimensional deconvolution and spectral unmixing software (CellR̂, version 3.0; Olympus Soft Imaging Solutions GmbH, Planegg, Germany).

DARPin selection. Ribosome display selection, expression, and purification of DARPins were performed as described previously (5, 31). All of the DARPins used in this study contain an N-terminal RGS-His_6 tag.

ELISAs. Epitope mapping was performed by enzyme-linked immunosorbent assay (ELISA) using immobilized biotinylated (Pierce EZ-Link Sulfo-NHS-LC-LC-Biotin; Thermo Scientific, Rockford, IL) recombinant VEGFR-2 ECD protein D1 to D7, D7, D1 to D3, or D2 to D4. ELISAs were developed with anti-RGS-His_6 horseradish peroxidase (HRP)-conjugated antibody (QIAgen, Hilden, Germany).

Competitive ELISA. Receptor specificity was established with biotinylated human VEGFR-2 (hVEGFR-2) D1 to D7 immobilized on neutravidin-coated, BSA-blocked Maxisorp plates (Nunc, Thermo Scientific, Roskilde, Denmark). DARPins (20 nM) were preincubated with 200 nM hVEGFR-1 (in-house), VEGFR-2 (in-house), hVEGFR-3 (Sino Biological, Beijing, China), mouse VEGFR-2 (mVEGFR-2; Sino Biological), human platelet-derived growth factor receptor β (hPDGFR-β; R&D Systems), or PBSTB (PBS with 0.1% Tween 20 and 0.5% BSA) for 2 h at RT in an end-over-end rotator. Solutions were applied to the ELISA plate for 20 min; this was followed by thorough washing and detection with an HRP-conjugated anti-RGS-His_6 antibody (Qiagen). Signals were normalized to the noncompeted signals.

DARPin affinity determination by SPR analysis. The kinetics of soluble DARPin binding to hVEGFR-2 were measured by surface plasmon resonance (SPR) analysis on a ProteOn XPR36 machine (Bio-Rad Laboratories, Hercules, CA). A GLC sensor chip (Bio-Rad Laboratories) was coated with neutravidin; this was followed by the immobilization of 850 resonance units of biotinylated hVEGFR-2 D1 to D7. Kinetic data were obtained by parallel injection of different concentrations of DARPins (6.25 to 100 nM) and buffer at a flow rate of 100 μl/min in PBS, pH 7.4, containing 0.005% Tween 20. Signals obtained with buffer only, as well as signals obtained with DARPins on a neutravidin-only surface, were subtracted. Data evaluation was performed with the ProteOn Manager software (Bio-Rad Laboratories).

SEC-MALS. Size exclusion chromatography-multiangle laser scattering (SEC-MALS) was used to determine the molecular weights of proteins and to assess complex formation by the ligand, receptor, and inhibitor. After system equilibration in 20 mM HEPES (pH 7.5), 150 mM NaCl at RT, samples were analyzed with three detectors in series, namely, UV and light-scattering detectors (Wyatt miniDAWN Tristar) coupled to a refractive-index detector (Optilab T-rEX refractometer; all from Wyatt Technology Corp., Wyatt Technology Europe GmbH, In der Steubach, Germany). Proteins in solution were routinely preincubated at 4°C for 45 min with DARPins in a 3× molar excess of ligand/receptor complex prior to characterization. Analysis was performed at RT by injecting a sample of 100 μg (1 mg/ml) into the SEC-MALS system (Superdex 200HR 10/30 column; GE Healthcare) in a mobile phase consisting of 20 mM HEPES (pH 7.5) and 150 mM NaCl at a flow rate of 0.5 ml/min. Data were analyzed and weight-averaged molar masses were calculated by using the ASTRA software (V5.1; Wyatt Technology).

Proliferation assay. PAEC or BAEC were plated at 6×10^3/well in 96-well plates. After adherence, cells were serum starved overnight and incubated in starvation medium containing 1 μM DARPin and 1.5 nM VEGF-A_{165} for 24 to 48 h. Subsequently, the medium was replenished with culture medium containing 20 μM resazurin and the cells were incubated for 2 to 4 h. The number of viable cells was obtained by monitoring resorufin fluorescence with a microplate spectrofluorometer (excitation wavelength, 544 nm; emission wavelength, 590 nm; ULTRA Evolution MultiDetection microplate reader and Magellan software V3.11; Tecan Group Ltd., Maennedorf, Switzerland).

Planar migration assay. The extent of gap closure of confluent PAEC or BAEC was assessed by scratch assay as previously described (18). Briefly, confluent cell cultures were scrape wounded and maintained in the presence or absence of 1.5 nM VEGF-A_{165} with or without DARPin (1 μM) for 24 to 48 h. Cell migration into the wounded area was scored as percent closure of the initial gap distance calculated from phase-contrast images taken with an Olympus IX81 microscope.

Chemotaxis assay. Transwell migration was assessed with Greiner Bio-one cell culture inserts 24 h after plating according to the manufacturer's instructions. Briefly, 0.8×10^6 PAEC or BAEC were seeded into translucent six-well inserts with an 8-μm pore size (Greiner Bio-one ThinCert; Huber & Co., Reinach, Switzerland) with or without a DARPin (1 μM) and the number of fluorescently labeled cells that migrated into the lower compartment containing a DARPin (1 μM) with or without VEGF-A_{165} at a concentration of 1.5 or 15 nM for BAEC or PAEC, respectively, was measured with a microplate spectrofluorometer (excitation wavelength, 485 nm; emission wavelength, 520 nm; ULTRA Evolution MultiDetection microplate reader and Magellan software V3.11; Tecan Group Ltd., Maennedorf, Switzerland).

Multicellular spheroid sprouting assay. Multicellular spheroids were prepared by the hanging-drop method (16). Briefly, cell suspensions of 500 to 800 cells in 30 μl of DMEM (10% FBS, 20% Methocel) were dispensed into large cell culture petri dishes using a multipipetter. Dishes were then inverted and incubated under standard conditions. After 24 h, 70 to 80 spheroids were pooled by centrifugation (relative centrifugal force, 100; 3 min) and suspended in 500 μl DMEM (10% FBS, 80% Methocel). In parallel, collagen solution (10% medium 199 [BioConcept], 80% collagen I stock, 2% 1 M HEPES, 8% 0.2 M NaOH) was prepared on ice. Spheroid suspensions were mixed 1:1 (vol/vol) with and without DARPins (0.1 to 1 μM) with collagen solution, transferred to prewarmed 24-well plates, and left to polymerize at 37°C for 2 h. Gels were overlaid with 500 μl of DMEM with or without VEGF-A_{165} to give a final concentration of 1.5 nM and incubated for 24 h. Spheroids were fixed with

3.7% formaldehyde at RT overnight and imaged. Spheroids were imaged using an Olympus IX81 phase-contrast microscope equipped with a 4× objective.

Statistical analysis. For statistical analysis of experimental data, multiple comparisons were investigated for significant differences by one-way analysis of variance. Individual comparisons were subsequently performed using the Bonferroni posttest or unpaired Student *t* test. Unless otherwise stated, data are expressed as means ± standard deviations, where *n* is the number of individual experiments; *P* values of ≤0.05 in two-sided tests were considered statistically significant (*, $P \leq 0.05$; **, $P \leq 0.001$; ***, $P \leq 0.0001$). All numerical and graphical analyses were performed in GraphPad Prism version 5.0 (GraphPad Software, San Diego, CA).

RESULTS

Ig domains D4 and D7 mutations reduce VEGFR-2 kinase activity. Our earlier published EM and SAXS analyses (14, 22) indicated that both D4 and D7 form homotypic contacts in receptor dimers. In addition, the crystal structure of ligand-bound c-Kit receptor dimers shows homotypic interactions via salt bridges between arginine and glutamate residues in the βE-F loop of D4 (30). Sequence alignment of type III and V RTKs shows that this dimerization motif is conserved and also present in D7 of VEGFR-2 (28) (Fig. 1B). To further investigate the importance of D7 in VEGFR-2 activation, we generated mutant constructs of VEGFR-2 D7 where single or multiple charged amino acids in the βE-F loop were replaced with alanine (Fig. 1C). The activities of these receptor constructs were determined by Western blotting with phospho- and VEGFR-2-specific antibodies using lysates prepared from VEGFR-2-expressing PAEC. The R726A mutant construct showed significant receptor kinase reduction by >55%, while the D731A mutant construct's activity was not significantly reduced (Fig. 2A and B). The xD7EF mutant construct, where all of the charged amino acids in the βE-F loop were mutated to alanine, lost >90% of its VEGF-inducible autophosphorylation activity (Fig. 2A and B). Single mutant constructs thus retained kinase activity, presumably because of compensatory interactions mediated by adjacent charged amino acids. These data, together with our earlier structural analysis (22) and the published VEGFR-2 D7 structure (28), suggest that the observed homotypic D7-D7 interaction is indeed indispensable for full VEGFR-2 activation. Since the role of D4 in VEGFR-2 had not been studied previously, we also generated a receptor mutant construct where D4 was replaced with D5 of VEGFR-1 (D3/5 mutant construct, Fig. 1C). Interestingly, this mutant construct was completely inactive in receptor kinase phosphorylation assays (Fig. 2A and B).

To confirm that our mutant receptors were correctly located at the cell membrane, we determined VEGFR-2 expression levels on the cell surface by immunofluorescence microscopy. Transiently transfected HEK293 cells were fixed and exposed to VEGFR-2 ECD-binding primary antibody, followed by a fluorescently conjugated secondary antibody. Figure 2C shows that all of the mutant receptor constructs are localized at the plasma membrane.

Taken together, these data show that both D4 and D7 are indispensable for VEGFR-2 activation and are presumably necessary to correctly position the intracellular kinase domains in active receptor dimers.

Isolation and characterization of Ig domain-specific DARPins. On the basis of the functional analysis of D4 and D7 mutant constructs, we selected DARPins (5) that bind to the recombinant VEGFR-2 ECD by using ribosome display. Out of 367 hits (hit rate, 30%), a total of 18 binding DARPins were chosen for further analysis. Eight of these DARPins bound D23, seven bound D7, and three bound elsewhere. Three DARPins that demonstrated inhibitory potential were chosen for detailed functional analysis, one each showing individual subdomain specificity for Ig domains D23 (inhibitor termed D23b), D4 (inhibitor termed D4b), and D7 (inhibitor termed D7b), respectively, as determined by ELISA using recombinant ECD proteins (Fig. 3A). In addition, these three DARPins were specific for hVEGFR-2 and did not cross-react with the related RTKs VEGFR-1, VEGFR-3, and PDGFR-β (Fig. 3B). Furthermore, DARPin D23b was species cross reactive with mVEGFR-2 ECD, albeit with a lower affinity (Fig. 3B). SPR analysis showed that all of the DARPins bound VEGFR-2 with high affinity and dissociation constants in the picomolar range, further corroborating the receptor specificity results obtained by competitive ELISA (Table 1).

To verify that these compounds also recognize native VEGFR-2 expressed on the surface of live cells, we performed immunofluorescence microscopy with receptor-expressing PAEC. Cells were fixed, permeabilized, incubated with a DARPin, and then incubated with a fluorescently labeled secondary antibody. All three DARPins recognized VEGFR-2 located on the cell surface (Fig. 3C). Our microscopic data thus document that the DARPins not only bind recombinant protein in ELISA and SPR analysis but also specifically recognize the properly folded native receptor expressed on the plasma membrane of live cells.

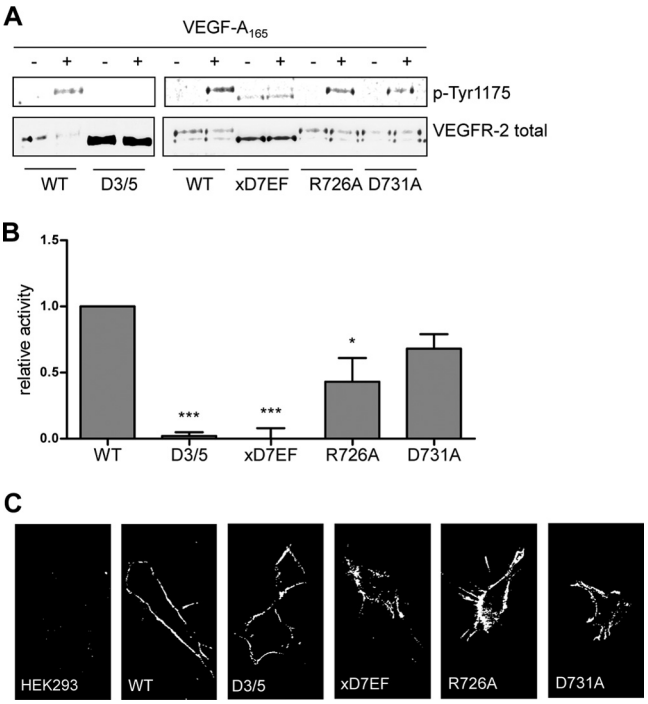

FIG 2 Ligand-induced activation of VEGFR-2 is reduced upon mutation of Ig domain D4 or D7. (A) Stably transfected PAEC expressing WT VEGFR-2, a D3/5 mutant construct, or R726A, D731A, and xD7EF D7 mutant constructs were stimulated with 1.5 nM VEGF-A_{165} for 10 min at 37°C. Receptor activity was determined by Western blot analysis with the antibodies indicated. (B) Quantification of receptor phosphorylation shown as *n*-fold increases over WT activity from triplicate experiments. (C) Immunofluorescence microscopy of HEK293 cells expressing WT or mutant VEGFR-2. Cells were stained with a VEGFR-2 ECD-specific antibody.

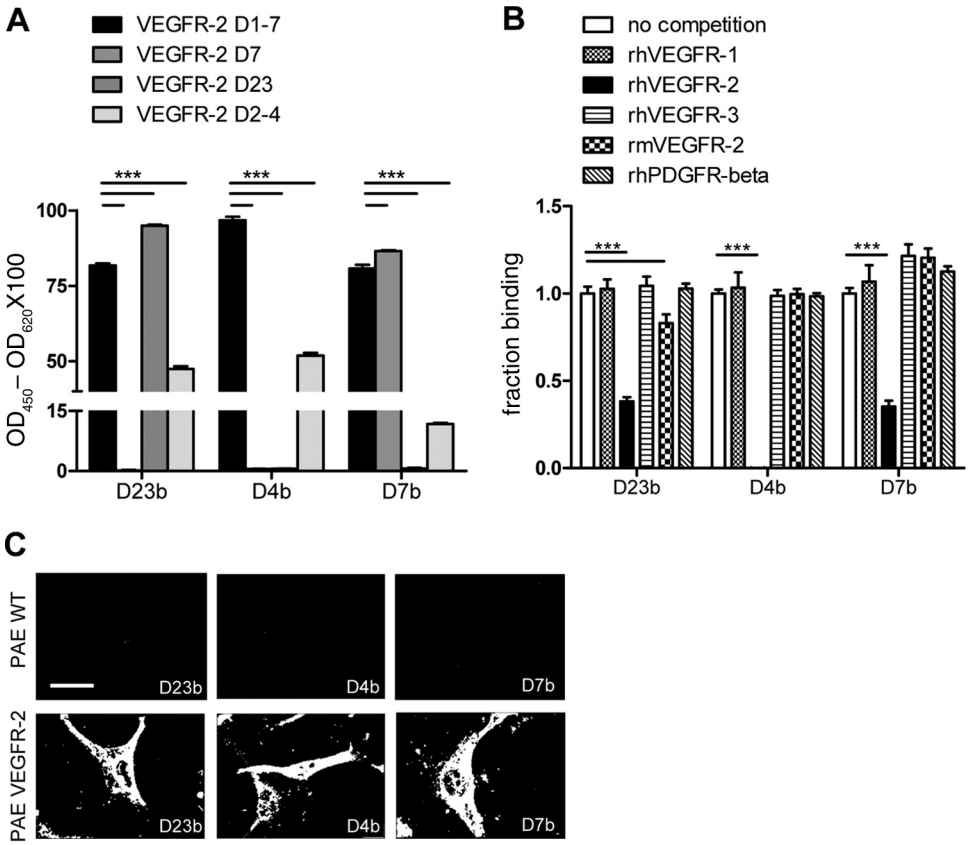

FIG 3 Characterization of DARPins binding to recombinant and native VEGFR-2 protein. (A) ELISA analysis to determine the VEGFR-2 Ig domain specificities of DARPins. OD_{450}, optical density at 450 nm. (B) Receptor binding specificities of DARPins for type III and V RTKs as determined by competitive ELISA. hVEGFR-2 D1 to D7 were immobilized on ELISA plates, and DARPin binding was measured in the absence (no competition) or presence of soluble competing receptor hVEGFR-1, hVEGFR-2, hVEGFR-3, mVEGFR-2, or hPDGFR-β, respectively. Signals are represented as fractions of the noncompeted signal obtained for each DARPin. (C) Immunofluorescence microscopy of VEGFR-2-bound DARPins on VEGFR-2-expressing PAEC. Cells were fixed and processed for immunofluorescence microscopy. Untreated cells were identically stained and used as controls (scale bar, 20 μm).

Effects of DARPins on ligand-mediated receptor dimerization. We next determined whether the DARPins impede ligand-mediated VEGFR-2 dimerization. Recombinant receptor ECD protein complexes were analyzed by SEC-MALS. Preformed complexes of D1 to D7 of VEGFR-2 and VEGF-A_{165} were analyzed by SEC-MALS in the presence or absence of DARPins. As expected, D23b competed for VEGF-A_{165} binding and disrupted preformed ligand/receptor complexes, as shown by the positions of the eluted proteins in the range of 200 and 100 kDa, representing receptor dimer and receptor monomers, respectively (Fig. 4A and B). DARPins D4b and D7b formed three-component protein complexes consisting of a receptor, a ligand, and a DARPin, as demonstrated by the increased M_r of the eluted peaks compared to the SEC-MALS data of the individually analyzed ligand and receptor protein (Fig. 4A). In addition, the presence of D4b and D7b did not lead to the dissociation of preformed ligand/receptor complexes, as documented by the chromatographic profiles showing peak protein elution at 230 and 224 kDa, respectively (Fig. 4A and Table 2). This was further confirmed by SDS-PAGE analysis of the peak protein fractions (Fig. 4B). Notably, the calculated M_r agreed with the theoretical values of the individual proteins (Table 2). Our data thus show that at least one molecule of D4b or D7b bound per ligand/receptor dimer. Taken together, these data show that D23b blocks ligand binding, and thus receptor dimerization, while D4b and D7b bind to receptor complexes but do not interfere with ligand-induced receptor dimerization.

TABLE 1 Kinetic parameters of anti-hVEGFR-2 DARPins[a]

DARPin	K_{on} (1/ms)	K_{off} (1/s)	K_d (nmol/liter)
D23b	4.44E-06	4.93E-05	0.01
D4b	5.63E-05	1.05E-04	0.19
D7b	3.80E-05	1.39E-04	0.37

[a] K_{on}, rate constant for association; K_{off}, rate constant for dissociation; K_d, dissociation constant (K_{off}/K_{on}).

Effects of DARPins on VEGFR-2 receptor activity. We next investigated whether DARPins interfere with receptor kinase activation. VEGFR-2-expressing PAEC were preincubated with DARPins for 45 min and then stimulated with VEGF-A_{165}. As shown in Fig. 5A and B, 1 μM D23b blocked receptor activity by >90%, and D4b and D7b inhibited it by >80%. Receptor inhibition was further documented by the reduction of ligand-induced PLCγ-1 phosphorylation by >90% (Fig. 5A and B). The inhibitory potential of all of the DARPins was already evident at a concentration of 100 nM, at which D23b inhibited by ≥90% and D4b and D7b inhibited by ≥40 to 60%. Combined treatment with D4b and D7b completely ablated phosphorylation at Tyr1175, demonstrating the synergistic inhibitory activity of these DARPins (data not

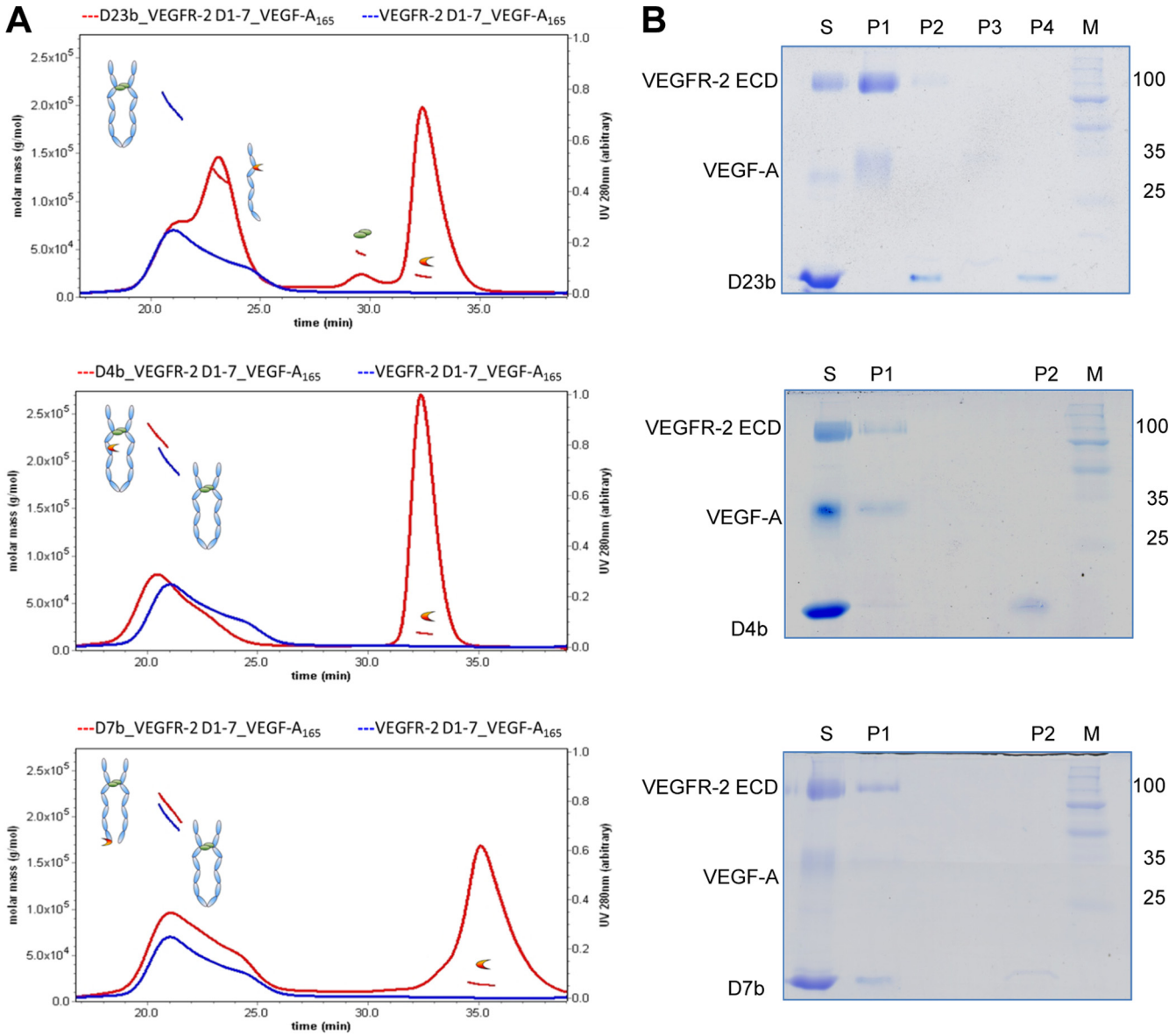

FIG 4 SEC-MALS analysis of the ligand/VEGFR-2 ECD complex in the presence of DARPins. Proteins in solution were incubated at 4°C for 30 min prior to analysis. (A) SEC-MALS analysis displaying weight-averaged molecular masses corresponding to SEC elution peaks for ligand/receptor complexes analyzed by MALS in the presence (red) and absence (blue) of DARPins. (B) The composition of the eluted fractions was analyzed in the order of elution by SDS-PAGE; S indicates sample before SEC, P1 to P4 refer to peaks in the chromatograms, and M shows molecular weight markers.

shown). Figure 5C shows the phosphorylation profile of all of the tyrosine residues in the kinase domain of the receptor. While phosphorylation of Tyr951, Tyr1054/59, and Tyr1175 was inhibited by all of the DARPins, Tyr1214 phosphorylation was upregulated even in the absence of a ligand, indicating differential regulation of receptor phosphorylation.

We next investigated the effects of DARPins on the activation of other downstream signaling targets of VEGFR-2. We determined the protein expression levels and activities of the mitogen-activated protein (MAP) kinases p38 and extracellular signal-regulated kinase 1/2 (ERK1/2) and of the lipid kinase target Akt. All three DARPins significantly inhibited ERK1/2 activity. Akt and p38 activities, however, are differently affected by DARPins; whereas DARPins induce downregulation of Akt activity, p38 shows ligand-independent upregulation (Fig. 6A and B). These activation profiles thus suggest that both p38 and Akt, but not ERK1/2 and PLCγ-1, are regulated via p-Tyr1214.

To exclude the possibility that toxic side effects were responsible for the inactivation of receptor signaling observed, we performed cell viability assays. All of the DARPins proved nontoxic at concentrations of 0 to 10 μM, with a cell viability of >90% (data not shown).

Functional characterization of DARPins. To conclude our analysis of the effects of ECD-targeting DARPins on VEGFR-2 signaling, we investigated their inhibitory potential in a series of functional assays in two endothelial cell lines. Our data show up to 67% inhibition of functional output in the presence of DARPins in cell proliferation (Fig. 7A) and planar cell migration (Fig. 7B),

TABLE 2 Schematic representations of MALS-analyzed proteins by structure and weight

Schematic representation	Protein(s) in complex	Theoretical atomic mass (kDa)		Avg molecular mass (kDa)	
		Monomer	Dimer	Monomer	Dimer
	VEGFR-2 D1 to D7	85		95	
	$VEGF\text{-}A_{165}$	15	30		30
	D23b/D4b	18		19	
	D7b	14		17	
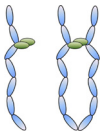	VEGFR-2 D1 to D7, $VEGF\text{-}A_{165}$	115	200		198
	D23b, VEGFR-2 D1 to D7	99–103		111	
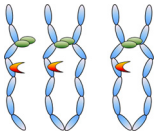	D4b, VEGFR-2 D1 to D7, $VEGF\text{-}A_{165}$	133	218–236	139	230
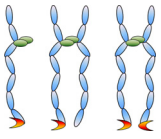	D7b, VEGFR-2 D1 to D7, $VEGF\text{-}A_{165}$	129	214–232	130	224

as well as up to 64% inhibition of VEGF-mediated chemotaxis (Fig. 7C) in VEGFR-2 PAEC and BAEC, compared to cells stimulated by $VEGF\text{-}A_{165}$ in the absence DARPins. The migration assays scrutinize two hallmarks of VEGF-mediated endothelial cell activation, namely, single-cell migration on a substrate and directional migration across an artificial membrane along a chemotactic gradient. Both assays thus show that DARPins, at concentrations of 0.1 μM in BAEC and 0.1 to 1 μM in VEGFR-2 PAEC, block cell migration (Fig. 7B and C). Finally, the effects of DARPins on angiogenic output were determined by *in vitro* sprouting assays performed with PAEC and BAEC. Multicellular spheroids were embedded in collagen gels, and $VEGF\text{-}A_{165}$-induced sprouting was quantified by assessing the number of sprouts per spheroid. All of the DARPins blocked the outgrowth of endothelial sprouts by >50% compared to the sprouting observed in spheroids under $VEGF\text{-}A_{165}$ treatment alone (Fig. 7D and E).

DISCUSSION

Here we show that the homotypic interactions in D4 and D7 previously described by EM (22), SAXS (14), and X-ray crystallography (29) are indispensable for full VEGFR-2 activation. These interactions seem to be mediated by conserved paired interactions of charged amino acids in the loop linking the βE with the βF strand in Ig domain D7. Point mutation of these residues gave rise to only partially defective receptors, presumably because of compensatory interactions mediated by adjacent charged amino acids. Mutation of all of the charged amino acids in the βE-F loop, however, completely blocked receptor activation and thus confirmed that these homotypic interactions are indispensable for ligand-mediated receptor activation. Our results partly contradict recently published functional data (28). Yang et al. showed that point mutations in the βE-F loop of D7 are sufficient to inhibit ligand-induced activation of VEGFR-2, whereas our data show that mutation of the entire loop is required to fully block receptor activation. This might be explained by the fact that Yang et al. used stably transfected, nonendothelial, VEGFR-2-expressing NIH 3T3 cells. In addition, they used chimeric receptor constructs consisting of the VEGFR-2 ECD fused to the intracellular kinase domain of the PDGFR, which may, because of structural inconsistencies, not adequately represent the performance of authentic VEGFR-2.

In agreement with our previous structural studies (14, 22) and with published work on VEGFR-1 (3), our study also demonstrates that mutation of Ig domain D4 completely inactivates VEGFR-2. Yang et al. identified a conserved amino acid sequence motif in Ig domain D4 of VEGFR-2, "D/E-X-G," which has high homology to the D4 dimerization motif of c-Kit (30) and PDGFR (29). It is therefore likely that the absence of this sequence in our D4 mutant construct disrupts homotypic D4 interactions. This is further confirmed by the results obtained with D4- and D7-specific DARPins discussed below, which clearly endorse an essential role for these domains in receptor activation and which suggest that these two membrane-

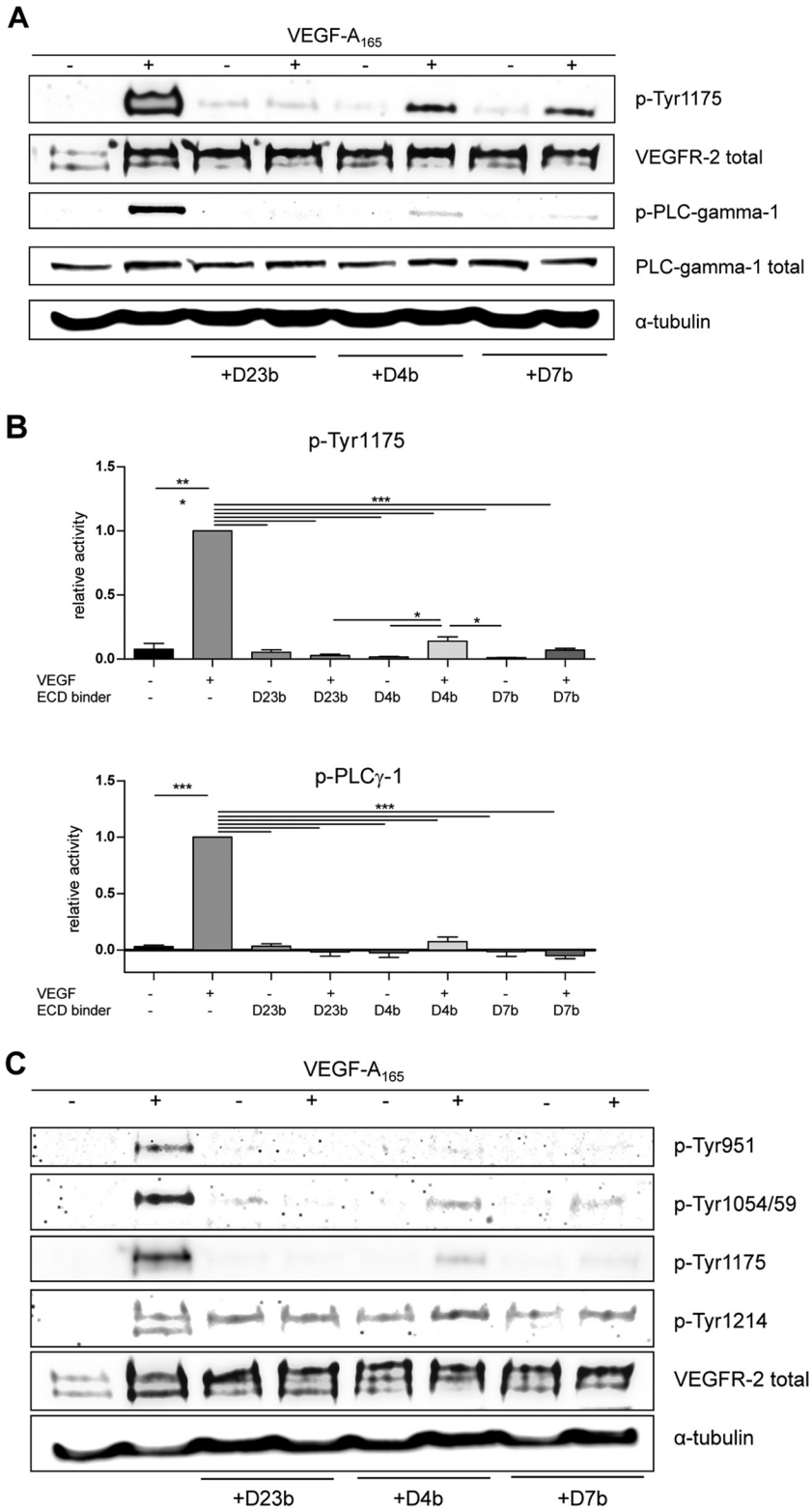

FIG 5 ECD binders inhibit VEGFR-2 activation and downstream signaling to PLCγ-1. (A) VEGFR-2 expressing PAEC were preincubated with ECD binders for 45 min and then stimulated with 1.5 nM VEGF-A_{165} for 10 min at 37°C. Receptor phosphorylation was analyzed by Western blot analysis with the antibodies indicated. (B) Quantification of Tyr1175 and PLCγ-1 phosphorylation is shown as *n*-fold increases over the activity of ligand-stimulated VEGFR-2 in the absence of inhibitors from three independent experiments. (C) Western blot analysis of major tyrosine residues of VEGFR-2.

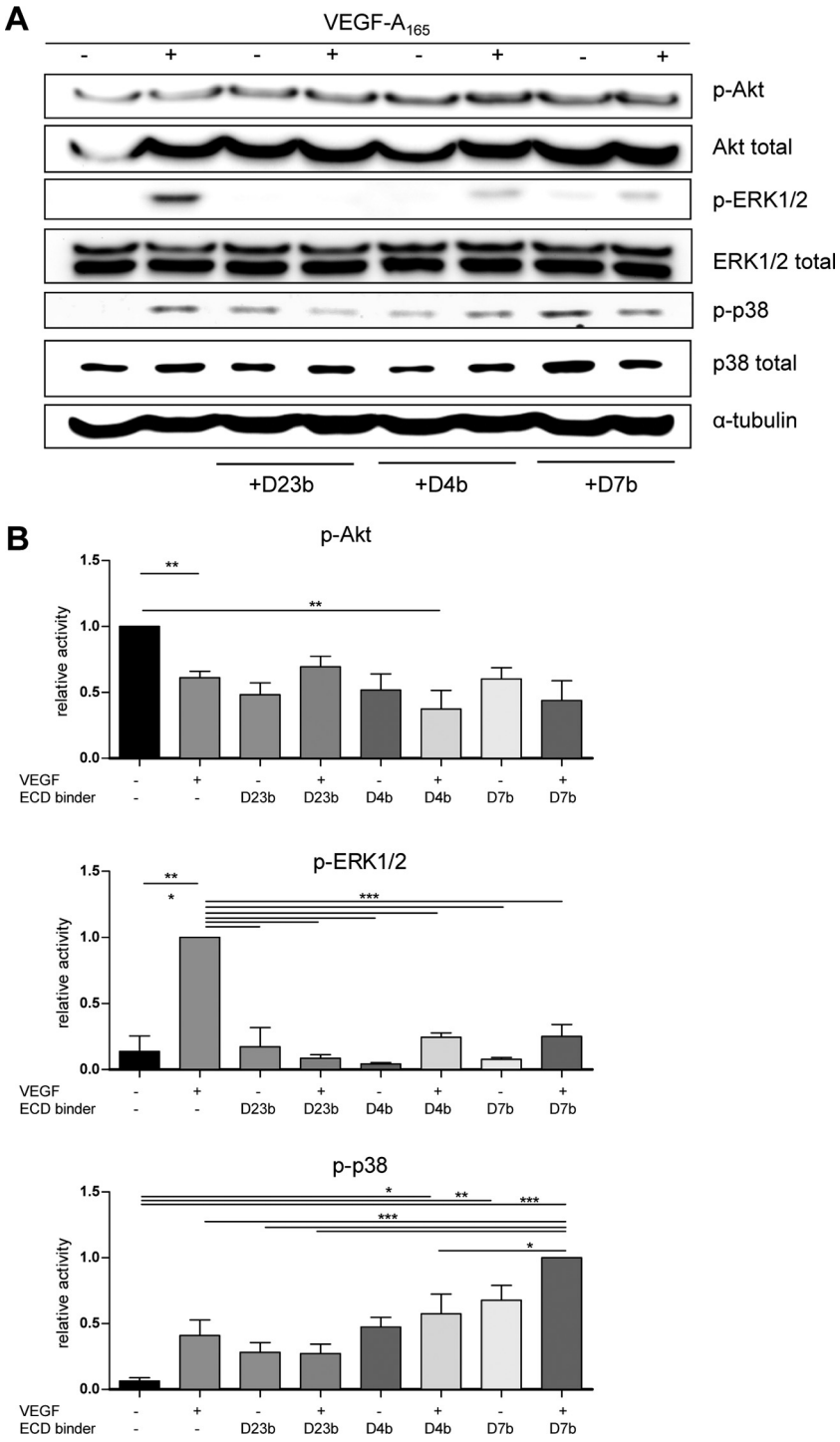

FIG 6 ECD binders inhibit VEGFR-2 signaling to MAP kinases and Akt. (A) VEGFR-2-expressing PAEC were preincubated with ECD binders for 45 min and then stimulated with 1.5 nM VEGF-A_{165} for 10 min at 37°C. VEGFR-2, p38, ERK1/2, and Akt phosphorylation was analyzed by Western blot analysis with the antibodies indicated. (B) Quantification of data is shown as *n*-fold increases in p38, ERK1/2, and Akt phosphorylation over the activity in ligand-stimulated cells in the absence of inhibitors from three independent experiments.

proximal Ig domains of the ECD act as allosteric regulatory sites in VEGFR-2 activation.

On the basis of our mutant construct analysis, we developed inhibitory DARPins specific for Ig domains D23, D4, and D7 of the VEGFR-2 ECD which effectively inhibited VEGFR-2 activity and downstream signaling. Incubating VEGFR-2-expressing cells with these inhibitors prior to VEGF-A_{165} stimulation drastically decreased receptor phosphorylation at Tyr951, Tyr1054/59, and Tyr1175 and inhibited signaling to downstream targets such as PLCγ-1 and ERK1/2. Akt activity was slightly increased under

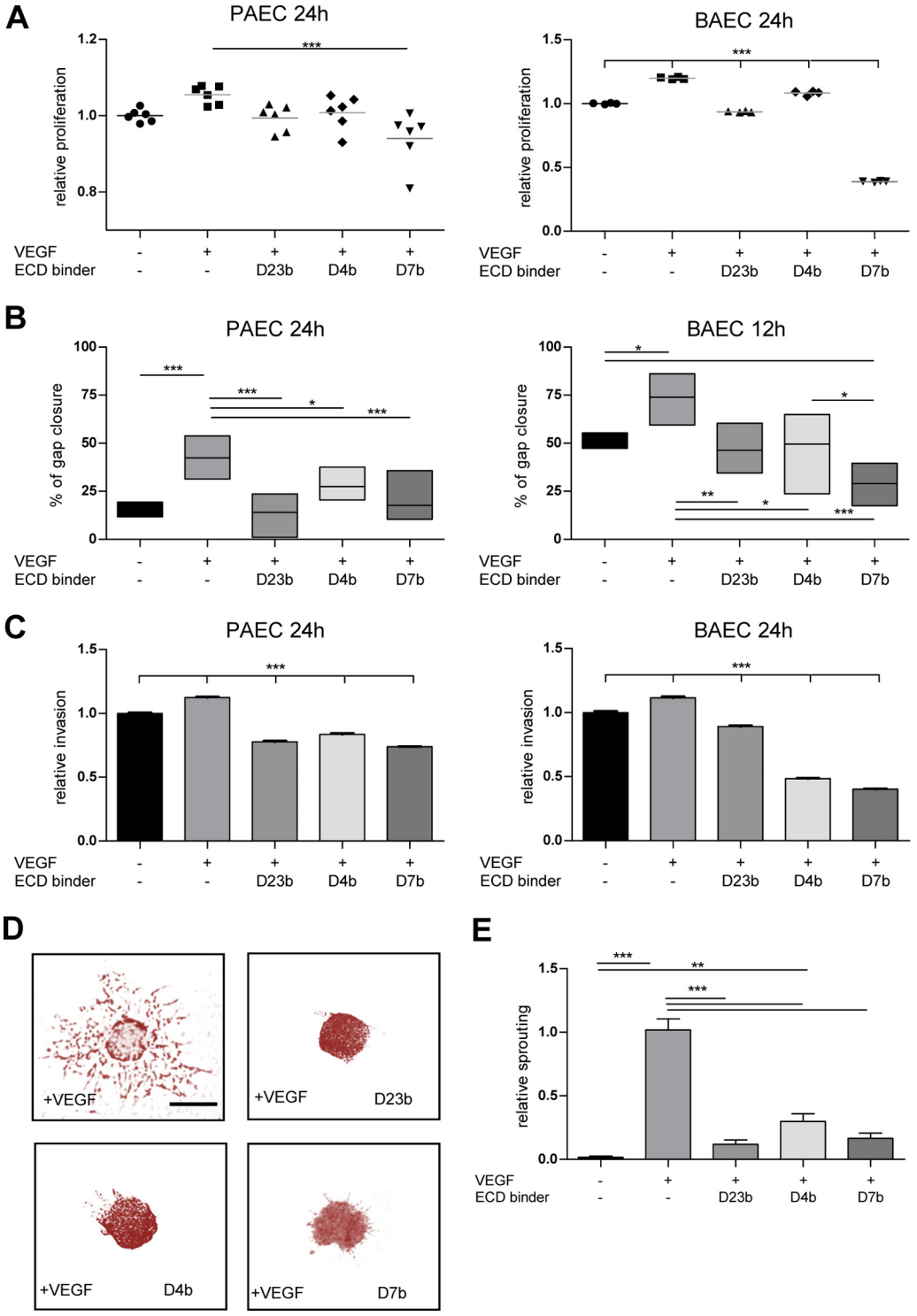

FIG 7 Inhibition of biological signal output by treatment with VEGFR-2 ECD-specific DARPins. Inhibition of proliferation (A), planar migration (B), and chemotaxis (C) in PAEC and BAEC is shown. (D) Sprouting of multicellular spheroids generated from VEGFR-2-expressing PAEC stimulated with 1.5 nM VEGF-A_{165}. Representative images of two independent experiments (scale bar, 200 μm). (E) The cumulative number of sprouts was analyzed morphometrically after 24 h in the presence or absence of inhibitors and is represented as relative intensity normalized to baseline sprouting.

these conditions. Most interestingly, DARPins activated, rather than inhibited, p38 MAP kinase activity even in the absence of a ligand, suggesting that p38 is downstream from p-Tyr1214. Phosphorylation of Tyr1214 is indeed upregulated by DARPins and apparently does not require VEGF stimulation. This unexpected behavior may, for instance, result from aberrant receptor trafficking induced by DARPin binding. The role of p38 in endothelial cell migration and proliferation may be antagonistic, as suggested

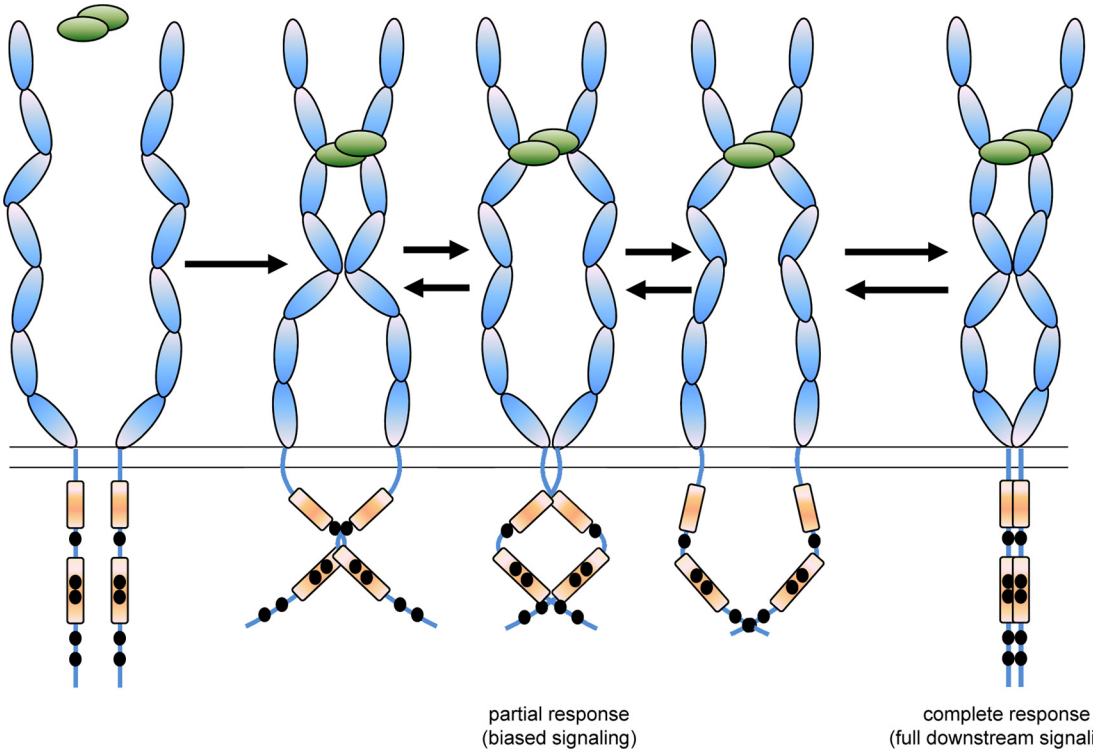

FIG 8 Model of VEGFR-2 activation. Ligand-mediated receptor dimerization at D23 together with homotypic receptor interactions at D4 and D7 position the intracellular kinase domains to instigate receptor phosphorylation at specific tyrosine residues. Interference with D4 and D7 interactions leads to "biased" signal output due to allosteric modulation of receptor dimer structure giving rise to partial cross- or transphosphorylation activity at selected tyrosine residues.

by Mullen et al., who showed that p38 activity is sufficient to promote cell migration but not proliferation (20). An investigation of the role of VEGF in promoting the activation of ERK1/2- and p38-specific phosphatases also showed that p38 is required for cell migration, while ERK1/2 elicited proliferative signals (4). Finally, it was shown that chemotactic migration of endothelial cells requires p38 activity (1, 19). An *in vitro* assay that reliably mimics angiogenic sprouting *in vivo* is the spheroid sprouting assay. Notably, all of the DARPins effectively blocked VEGF-A_{165}-induced endothelial cell spheroid sprouting.

Earlier data published by Tao et al. showed that membrane-proximal D4 to D7 blocked receptor dimerization and activation and are thus essential for maintaining the receptor in an inactive conformation in the absence of a ligand (26). This is in agreement with our recent data showing that D4 to D7 indeed attenuate ligand binding affinity and may thereby safeguard VEGFR-2 against aberrant ligand-independent activation (6). Taken together, these data suggest that both D4 and D7 are required to correctly position the intracellular kinase domains relative to each other to allow the activation of ligand-bound dimeric receptors (7). These findings are prominently supported by our SEC-MALS analysis of protein complex formation, which provides insight into the molecular mechanism of receptor inhibition by the D4- and D7-specific DARPins. Although D4b and D7b do not block receptor dimerization, they seem to obstruct the correct three-dimensional organization of receptor monomers in ligand-bound dimers. This not only leads to profound inhibition of receptor activity but also seems to redirect signal output to distinct signaling pathways and may thus cause "biased" receptor signal output, as summarized in a schematic model in Fig. 8.

The advantages of the D4- and D7-targeting DARPins over inhibitors that interact with the kinase or receptor ligand-binding domain are their high target specificity and noncompetitive binding mode. In this study, we have thus identified a novel and potent inhibitory mechanism for VEGFR-2. This newly identified function of the membrane-proximal ECDs in receptor kinase regulation may be generally applicable to all type III and V RTKs. In a similar fashion, a monoclonal antibody against D5 of VEGFR-3 that blocks VEGFR-2/VEGFR-3 heterodimerization was shown to suppress signal transduction, migration, and sprouting of microvascular endothelial cells (27). Finally, Kendrew et al. generated a human antibody in a XenoMouse which binds between D4 and D7 and suppresses VEGFR-2 activation (13); however, the mode of action of this antibody has so far not been further specified. Finally, a mechanistically similarly acting inhibitor currently in clinical trials is Pertuzumab (8a), which blocks ErbB2 heterodimerization with other members of the ErbB receptor family.

In summary, we have shown that D4 and D7 are indispensable for ligand-mediated VEGFR-2 activation. Our data shed new light on the interdependencies of receptor ECD structure and intracellular kinase activity and identify key targets for the design of new VEGFR-2 inhibitors. Furthermore, we show that D4- and D7-specific DARPins demonstrate high receptor specificity and excellent binding affinities. These reagents represent novel allosteric receptor regulators applicable to all type III and V RTKs. In a next

step, we hope to show efficacy in preclinical *in vivo* applications such as antiangiogenic therapies or medical diagnostics.

ACKNOWLEDGMENTS

We thank Nathalie Fahrer-Lau for technical support and Daniel Steiner for helpful discussions.

We thank the Swiss National Science Foundation (grants 31003A-130463 issued to K.B.-H. and PMCDP3-134208/1 issued to C.A.C.H.), Oncosuisse (grant OC2 01200-08-2007 issued to K.B.-H.), and the Novartis Stiftung für medizinisch-biologische Forschung (grant 10C61 issued to K.B.-H.) for generous support of this work.

REFERENCES

1. **Arefieva TI, Kukhtina NB, Antonova OA, Krasnikova TL.** 2005. MCP-1-stimulated chemotaxis of monocytic and endothelial cells is dependent on activation of different signaling cascades. Cytokine **31**:439–446.
2. **Aricescu AR, Lu W, Jones EY.** 2006. A time- and cost-efficient system for high-level protein production in mammalian cells. Acta Crystallogr. D Biol. Crystallogr. **62**:1243–1250.
3. **Barleon B, et al.** 1997. Mapping of the sites for ligand binding and receptor dimerization at the extracellular domain of the vascular endothelial growth factor receptor FLT-1. J. Biol. Chem. **272**:10382–10388.
4. **Bellou S, et al.** 2009. VEGF autoregulates its proliferative and migratory ERK1/2 and p38 cascades by enhancing the expression of DUSP1 and DUSP5 phosphatases in endothelial cells. Am. J. Physiol. Cell Physiol. **297**:C1477–C1489.
5. **Binz HK, et al.** 2004. High-affinity binders selected from designed ankyrin repeat protein libraries. Nat. Biotechnol. **22**:575–582.
6. **Brozzo MS, et al.** 2012. Thermodynamic and structural description of allosterically regulated VEGF receptor 2 dimerization. Blood **119**:1781–1788.
7. **Dell'Era Dosch D, Ballmer-Hofer K.** 2010. Transmembrane domain-mediated orientation of receptor monomers in active VEGFR-2 dimers. FASEB J. **24**:32–38.
8. **Eriksson A, et al.** 2003. Small GTP-binding protein Rac is an essential mediator of vascular endothelial growth factor-induced endothelial fenestrations and vascular permeability. Circulation **107**:1532–1538.

8a. **Franklin MC, et al.** 2004. Insights into ErbB signaling from the structure of the ErbB2-pertuzumab complex. Cancer Cell **5**:317–328.

9. **Fuh G, Li B, Crowley C, Cunningham B, Wells JA.** 1998. Requirements for binding and signaling of the kinase domain receptor for vascular endothelial growth factor. J. Biol. Chem. **273**:11197–11204.
10. **Geiser M, Cébe R, Drewello D, Schmitz R.** 2001. Integration of PCR fragments at any specific site within cloning vectors without the use of restriction enzymes and DNA ligase. Biotechniques **31**:88–90, 92.
11. **Graham FL, Smiley J, Russell WC, Nairn R.** 1977. Characteristics of a human cell line transformed by DNA from human adenovirus type 5. J. Gen. Virol. **36**:59–74.
12. **Heinzel SS, Krysan PJ, Calos MP, DuBridge RB.** 1988. Use of simian virus 40 replication to amplify Epstein-Barr virus shuttle vectors in human cells. J. Virol. **62**:3738–3746.
13. **Kendrew J, et al.** 2011. An antibody targetted to VEGFR-2 Ig domains 4-7 inhibits VEGFR-2 activation and VEGFR-2 dependent angiogenesis without affecting ligand binding. Mol. Cancer Ther. **10**:770–783.
14. **Kisko K, et al.** 2011. Structural analysis of vascular endothelial growth factor receptor-2/ligand complexes by small-angle X-ray solution scattering. FASEB J. **25**:2980–2986.
15. **Koch S, Tugues S, Li X, Gualandi L, Claesson-Welsh L.** 2011. Signal transduction by vascular endothelial growth factor receptors. Biochem. J. **437**:169–183.
16. **Korff T, Krauss T, Augustin HG.** 2004. Three-dimensional spheroidal culture of cytotrophoblast cells mimics the phenotype and differentiation of cytotrophoblasts from normal and preeclamptic pregnancies. Exp. Cell Res. **297**:415–423.
17. **Leppänen VM, et al.** 2010. Structural determinants of growth factor binding and specificity by VEGF receptor 2. Proc. Natl. Acad. Sci. U. S. A. **107**:2425–2430.
18. **Liang CC, Park AY, Guan JL.** 2007. In vitro scratch assay: a convenient and inexpensive method for analysis of cell migration in vitro. Nat. Protoc. **2**:329–333.
19. **Liu F, et al.** 2001. Differential regulation of sphingosine-1-phosphate- and VEGF-induced endothelial cell chemotaxis. Involvement of G(ialpha2)-linked Rho kinase activity. Am. J. Respir. Cell Mol. Biol. **24**:711–719.
20. **McMullen ME, Bryant PW, Glembotski CC, Vincent PA, Pumiglia KM.** 2005. Activation of p38 has opposing effects on the proliferation and migration of endothelial cells. J. Biol. Chem. **280**:20995–21003.
21. **Pepper MS, et al.** 1992. Coupling and connexin 43 expression in microvascular and large vessel endothelial cells. Am. J. Physiol. **262**:C1246–C1257.
22. **Ruch C, Skiniotis G, Steinmetz MO, Walz T, Ballmer-Hofer K.** 2007. Structure of a VEGF-VEGF receptor complex determined by electron microscopy. Nat. Struct. Mol. Biol. **14**:249–250.
23. **Ruch C.** 2007. Structure/function analysis of the extracellular domain of vascular endothelial growth factor receptor-2 (VEGFR-2). Ph.D. dissertation. ETH, Zurich, Switzerland.
24. **Shinkai A, et al.** 1998. Mapping of the sites involved in ligand association and dissociation at the extracellular domain of the kinase insert domain-containing receptor for vascular endothelial growth factor. J. Biol. Chem. **273**:31283–31288.
25. **Stuttfeld E, Ballmer-Hofer K.** 2009. Structure and function of VEGF receptors. IUBMB Life **61**:915–922.
26. **Tao Q, Backer MV, Backer JM, Terman BI.** 2001. Kinase insert domain receptor (kdr) extracellular immunoglobulin-like domains 4-7 contain structural features that block receptor dimerization and vascular endothelial growth factor-induced signaling. J. Biol. Chem. **276**:21916–21923.
27. **Tvorogov D, et al.** 2010. Effective suppression of vascular network formation by combination of antibodies blocking VEGFR ligand binding and receptor dimerization. Cancer Cell **18**:630–640.
28. **Yang Y, Xie P, Opatowsky Y, Schlessinger J.** 2010. Direct contacts between extracellular membrane-proximal domains are required for VEGF receptor activation and cell signaling. Proc. Natl. Acad. Sci. U. S. A. **107**:1906–1911.
29. **Yang Y, Yuzawa S, Schlessinger J.** 2008. Contacts between membrane proximal regions of the PDGF receptor ectodomain are required for receptor activation but not for receptor dimerization. Proc. Natl. Acad. Sci. U. S. A. **105**:7681–7686.
30. **Yuzawa S, et al.** 2007. Structural basis for activation of the receptor tyrosine kinase KIT by stem cell factor. Cell **130**:323–334.
31. **Zahnd C, Amstutz P, Pluckthun A.** 2007. Ribosome display: selecting and evolving proteins in vitro that specifically bind to a target. Nat. Methods **4**:269–279.